An Improved Toeplitz Approximation Method for Coherent DOA Estimation in Impulsive Noise Environments

Jiang'an Dai [1], **Tianshuang Qiu** [1,*], **Shengyang Luan** [2], **Quan Tian** [3] **and Jiacheng Zhang** [4]

1   Faculty of Electronic Information and Electrical Engineering, Dalian University of Technology, Dalian 116024, China
2   School of Electrical Engineering and Automation, Jiangsu Normal University, Xuzhou 221116, China
3   School of Electronics and Information Engineering, Taizhou University, Taizhou 318000, China; tianquan10@163.com
4   School of Artificial Intelligence, Nanjing University of Information Science and Technology, Nanjing 210000, China
*   Correspondence: qiutsh@dlut.edu.cn; Tel.: +86-0411-84709573

Abstract: Direction of arrival (DOA) estimation is an important research topic in array signal processing and widely applied in practical engineering. However, when signal sources are highly correlated or coherent, conventional subspace-based DOA estimation algorithms will perform poorly due to the rank deficiency in the received data covariance matrix. Moreover, conventional DOA estimation algorithms are usually developed under Gaussian-distributed background noise, which will deteriorate significantly in impulsive noise environments. In this paper, a novel method is presented to estimate the DOA of coherent signals in impulsive noise environments. A novel correntropy-based generalized covariance (CEGC) operator is defined and proof of boundedness is given to ensure the effectiveness of the proposed method in impulsive noise environments. Furthermore, an improved Toeplitz approximation method combined CEGC operator is proposed to estimate the DOA of coherent sources. Compared to other existing algorithms, the proposed method can avoid array aperture loss and perform more effectively, even in cases of intense impulsive noise and low snapshot numbers. Finally, comprehensive Monte-Carlo simulations are performed to verify the superiority of the proposed method under various impulsive noise conditions.

Keywords: direction of arrival estimation; coherent signals; impulsive noise; correntropy; generalized covariance; Toeplitz approximation

1. Introduction

As a fundamental component of array signal processing, direction of arrival (DOA) estimation has been continuously attracting much attention from researchers and been widely applied in numerous fields such as radar, sonar, satellite navigation, wireless communications, and biomedicine [1–5]. After decades of research, various high-resolution DOA estimation methods have been proposed [6]. Among them, the subspace-based methods are well-known and effective. Utilizing eigenvalue decomposition (EVD) or singular value decomposition (SVD), the subspace-based methods can partition received data covariance matrices into signal subspace and noise subspace. Based on specific properties of subspace, such as orthogonality and rotational invariance, many high-resolution methods have been proposed, such as multiple signal classification (MUSIC) [7], estimation of signal parameters via rotational invariance techniques (ESPRIT) [8] and subspace fitting methods [9].

Compared to other conventional DOA estimation methods such as the maximum likelihood (ML) methods [10], the subspace-based methods are relatively computationally efficient and highly practical. Thus, the subspace-based methods have been widely studied

and many variants have been proposed over the past several years. However, the subspace-based methods were originally proposed for uncorrelated signals for which the rank of the data covariance matrix is equal to the number of signal sources. When the signal sources are highly correlated or coherent, these methods will encounter significant difficulties. Signal coherence is a common phenomenon that can be caused by natural multipath propagation effects or intentional hostile jamming. This will in turn result in a rank deficiency in the source covariance matrix and a divergence of the signal eigenvector into the noise subspace. Therefore, conventional subspace-based methods may produce several pseudo peaks and fail to accurately perform DOA estimation, particularly when the signal sources are close together.

To eliminate the adverse effects caused by signal coherence, numerous methods have been proposed [11–27]. A well-known method known as spatial smoothing (SS) or forward-only spatial smoothing (FOSS) was proposed in Evans et al. [11] to estimate DOA regardless of the coherence of signal sources, and a detailed analysis of the SS method was given in Shan et al. [12]. The main concept of the SS technique is to partition the entire received array into several overlapped subarrays and obtain a modified signal covariance matrix through subarray averaging. The SS technique can be seen as a preprocessing procedure to de-correlate the received signals and resolve DOA estimation of coherent sources when combined with the subspace-based methods. However, the SS technique does not fully utilize the useful information in the signal covariance matrix. Moreover, the effective aperture of the array is significantly reduced due to the subarray's partition and average operation, which means the number of coherent signals that can be detected is significantly reduced. To circumvent these problems, several modified SS methods have been proposed [13–19]. In Williams et al. [13], an improved SS method called forward/backward spatial smoothing (FBSS) was developed to reduce aperture loss. The FBSS method utilizes both forward subarrays and complex conjugated backward subarrays to improve the performance and is able to estimate any K DOAs using $3K/2$ sensor elements, while the SS method requires $2K$ sensor elements by contrast. Li [15] examined the performance of the SS as well as the FBSS method and showed that the angular resolution can be enhanced by squaring array covariance matrices. In Du and Kirlin [17], an improved spatial smoothing method that can fully utilize the correlations of array outputs was presented. Pan et al. [19] proposed an enhanced spatial smoothing (ESS) technique that fully exploits the information of both the covariance matrices and cross-covariance matrices of the subarrays. Although these modified SS methods can improve the performance of the SS method to a certain extent, the problem of aperture loss remains unresolved.

In addition to the SS-based methods, the Toeplitz approximation method (TAM) [20] is an alternative to circumvent problems encountered in the DOA estimation of coherent signals. The TAM method is proposed based on the fact that the covariance matrix of uncorrelated stationary sources is Toeplitz and can reconstruct the covariance matrix of coherent sources with Toeplitz structure. Compared to the SS method, the TAM method does not reduce the effective aperture of the array and has higher resolution capability. In Chen et al. [22], a modification of the TAM and an iterative version of the TAM were used for bearing estimation with sensor location errors. Han et al. [23] proposed an ESPRIT-like algorithm based on Toeplitz matrix reconstruction. This method can achieve accurate estimation performance with low computational complexity; however, the method requires additional array elements. In Qian et al. [24], a coherent DOA estimation scheme was proposed to solve the optimization problem based on a newly designed cost function. This scheme can adequately exploit the information of the reconstructed Toeplitz matrix and work properly without a priori information, such as the source number. Zhang et al. [25] proposed a multiple Toeplitz matrices reconstruction method for coherent DOA estimation that adequately applied information contained in the correlation matrices. In Zhang et al. [26], a modified method called forward and backward partial Toeplitz matrices reconstruction (FB-PTMR) was proposed, which exploits half of the array covariance matrix to reconstruct data in a Toeplitz matrix. The FB-PTMR can overcome the drawbacks of other methods due to

its neglect of phase differences and utilize more information compared to the ESPRIT-like algorithm. Dai et al. [27] proposed a coherent DOA estimation scheme combining full-row Toeplitz matrices reconstruction and deep learning network architecture to achieve higher performance with lower computational cost.

The coherent DOA estimation methods mentioned above assume that ambient noise is Gaussian-distributed. In reality, however, there are various non-Gaussian noises with spike impulse characteristics [28–30], such as atmospheric noise, underwater noise, vehicle ignition, multi-user interference, etc. These impulsive noises usually have heavy-tailed distributions, which means the probability density function (PDF) decreases more slowly and outliers are more likely to occur compared to Gaussian distribution. Under the impulsive noise environment, the performance of the above coherent DOA estimation methods will severely degrade. Therefore, an appropriate distribution method is needed to model the impulse noise. There are multiple non-Gaussian distributions used to characterize impulsive noise with heavy-tailed PDFs, such as generalized Gaussian distribution [31], Gaussian mixture distribution [32], and alpha-stable (α-stable) distribution [28,33]. Among these distributions, only α-stable distribution satisfies the generalized central limit theorem [33]. Meanwhile, α-stable distribution could provide a connection between Gaussian and non-Gaussian distribution. In fact, Gaussian distributions and various non-Gaussian distributions are special cases of the α-stable distribution family. Therefore, α-stable distribution is an appropriate model for impulsive noise.

Some studies have been devoted to the problem of coherent DOA estimation in the presence of impulsive noise. In Visuri et al. [34], two nonparametric DOA estimation algorithms were presented in the presence of non-Gaussian noise and multipath propagation effects. These algorithms are based on multivariate spatial sign covariance matrices and combined with SS to deal with coherent sources. The theoretical analysis and some extensions of the algorithms are then given in Visuri et al. [35]. Rupi et al. [36] combined a signed-power nonlinearity and SS to mitigate the effects of the heavy-tailed background noise and reduce the measured coherence. In Li et al. [37], novel algorithms based on fractional lower-order statistics (FLOS) and FBSS were proposed for DOA estimation of coherent sources in the presence of impulsive noise. Liu et al. [38] presented an algorithm which combined SS and infinity-norm normalization (INF) to estimate the DOA of coherent sources in impulsive noise environments. In Li and Lin [39], SS was applied to the phased fractional lower order moments (PFLOM) matrices and a robust algorithm called PFLOM-SS was proposed for DOA estimation of coherent sources under impulsive noise environments. Guan et al. [40] defined and compared three different decorrelation methods for DOA estimation of coherent sources based on correntropy-based correlation (CRCO). These improved SS-based methods can alleviate performance degradation to a certain extent, but they share the inherent disadvantages of the SS-based algorithm, that is, the effective aperture array will be reduced. Meanwhile, the performance of these methods will deteriorate significantly when the ambient noise is highly impulsive, and the number of snapshots is low. Therefore, further studies are required to adequately address the problem of DOA estimation of coherent signals under impulsive noise.

In this paper, a new coherent DOA estimation method based on correntropy-based generalized covariance (CEGC) and Toeplitz approximation are presented. The remainder of this paper is organized as follows. Section 2 presents some preliminary knowledge related to our method, including the signal model and noise model. In Section 3, the procedure of the proposed method is briefly introduced. In Section 4, Monte-Carlo simulations are carried out to evaluate the performance of the proposed and other existing methods under different conditions. Conclusions are finally drawn in Section 5.

Notation: Matrices, vectors, and scalar quantities are denoted by uppercase boldface, lowercase boldface, and lowercase letters, respectively. $(\cdot)^*$, $(\cdot)^T$, and $(\cdot)^H$ denote conjugate, transpose, and conjugate transpose, respectively. $\text{diag}(\cdot)$ denotes diagonal matrix. $\delta(\cdot)$ denotes the Dirac delta function. $|\cdot|$ denotes absolute value operation. $\max(\cdot)$ denotes maximum operation. $\text{E}(\cdot)$ denotes the mathematic expectation operation.

2. Preliminaries

2.1. Signal Model of Coherent DOA Estimation

Consider a uniform linear array (ULA) consisting of M omnidirectional sensors receiving K narrow-band plane-wave signals from directions $\{\theta_1, \theta_2, \ldots, \theta_K\}$, where θ_k denotes the DOA of the kth signal source.

Due to the effect of multipath propagation and other factors, there is usually a certain degree of correlation between two signal sources. The correlation coefficient ρ_{ij} between $x_i(t)$ and $x_j(t)$ indicates the degree of correlation and can be written as:

$$\rho_{ij} = \frac{\mathrm{E}\left[x_i(t)x_j^*(t)\right]}{\sqrt{\mathrm{E}\left[|x_i(t)|^2\right]\mathrm{E}\left[|x_j(t)|^2\right]}} \tag{1}$$

According to the Cauchy–Schwarz inequality, we know that $|\rho_{ij}| \leq 1$. When $\rho_{ij} = 0$, $x_i(t)$ and $x_j(t)$ are uncorrelated. When $0 < |\rho_{ij}| < 1$, $x_i(t)$ and $x_j(t)$ are (partially) correlated. When $|\rho_{ij}| = 1$, $x_i(t)$ and $x_j(t)$ are coherent (completely correlated).

If the K signal sources $\{x_1(t), x_2(t), \ldots, x_K(t)\}$ are coherent, taking the first signal $x_1(t)$ as the reference, the kth signal source at time t can be represented as

$$x_k(t) = A_k x_1(t), k = 1, 2, \ldots, K \tag{2}$$

where A_k denotes the complex attenuation of the kth signal with respect to $x_1(t)$. Then the signal sources matrix can be represented as:

$$\boldsymbol{X} = [\boldsymbol{x}(1), \boldsymbol{x}(2), \ldots, \boldsymbol{x}(N)] \tag{3}$$

where N is the number of snapshots. $\boldsymbol{x}(t) = [x_1(t), x_2(t), \ldots, x_K(t)]^{\mathrm{T}}$ represents the signal sources vector.

The array manifold matrix can be represented as:

$$\boldsymbol{A} = [\boldsymbol{a}(\theta_1), \boldsymbol{a}(\theta_2), \ldots, \boldsymbol{a}(\theta_K)] \tag{4}$$

where $\boldsymbol{a}(\theta_k) = [a_1(\theta_k), a_2(\theta_k), \ldots, a_M(\theta_k)]^{\mathrm{T}}$ represents the steering vector of the kth signal source. $a_m(\theta_k) = e^{\mathrm{j}2\pi \sin\theta_k(m-1)d/\lambda}$ represents the component of $\boldsymbol{a}(\theta_k)$ corresponding to the mth sensor. d is the spacing between two adjacent sensors. λ is the wavelength.

Using complex signal representation, the received signal $y_m(t)$ at the mth sensor can be represented as:

$$y_m(t) = \sum_{k=1}^{K} x_k(t)a_m(\theta_k) + w_m(t), \quad m = 1, 2, \ldots, M \tag{5}$$

where $w_m(t)$ represents the noise at the mth sensor.

Then the received signal matrix can be represented as:

$$\boldsymbol{Y} = [\boldsymbol{y}(1), \boldsymbol{y}(2), \ldots, \boldsymbol{y}(N)] \tag{6}$$

where $\boldsymbol{y}(t) = [y_1(t), y_2(t), \ldots, y_M(t)]^{\mathrm{T}}$ represents the received signal vector.

Moreover, Equation (5) can be represented more compactly in matrix form as:

$$\boldsymbol{Y} = \boldsymbol{A}\boldsymbol{X} + \boldsymbol{W} \tag{7}$$

where $\boldsymbol{W} = [\boldsymbol{w}(1), \boldsymbol{w}(2), \ldots, \boldsymbol{w}(N)]$ denotes the received noise matrix. $\boldsymbol{w}(t) = [w_1(t), w_2(t), \ldots, w_M(t)]^{\mathrm{T}}$ represents the received noise vector. The purpose of this paper is utilizing noisy received data $\boldsymbol{Y}$ to estimate the DOA $\{\theta_1, \theta_2, \ldots, \theta_K\}$ of K coherent signal sources $\{x_1(t), x_2(t), \ldots, x_K(t)\}$.

2.2. α-Stable Distribution Noise Model

The α-stable distribution is an appropriate model of non-Gaussian impulsive noise due to its generality. Since there is no closed-form expression for its PDF, α-stable distribution is usually described by its characteristic function. The characteristic function of α-stable distribution can be represented as in Shao and Nikias [33]:

$$\phi(\omega) = e^{j\mu\omega - \gamma|\omega|^{\alpha}[1+j\beta\mathrm{sgn}(\omega)\zeta(\omega,\alpha)]} \tag{8}$$

$$\mathrm{sgn}(\omega) = \begin{cases} 1 & ,\omega > 0 \\ 0 & ,\omega = 0 \\ -1 & ,\omega < 0 \end{cases} \tag{9}$$

$$\zeta(\omega,\alpha) = \begin{cases} \tan\frac{\pi\alpha}{2}, \alpha \neq 1 \\ \frac{2}{\pi}\log|\omega|, \alpha = 1 \end{cases} \tag{10}$$

where $\mu \in (-\infty, +\infty)$ is the location parameter. $\alpha \in (0, 2]$ is the characteristic exponent, and it measures the thickness of the tails of the PDF. When $\alpha = 2$, α-stable distribution is equivalent to Gaussian distribution. With the decrease of α, the noise will behave more impulsively. $\beta \in [-1, 1]$ is the symmetry parameter. When $\beta = 0$, the distribution is symmetric about the center μ and is called symmetric alpha-stable ($S\alpha S$) distribution. $\gamma \in (0, +\infty)$ is the dispersion parameter and plays a role similar to that of the variance for Gaussian distribution.

In this paper, we utilize the $S\alpha S$ distribution to model impulsive noise. Therefore, (8) can be simplified as:

$$\phi(\omega) = e^{j\mu\omega - \gamma|\omega|^{\alpha}} \tag{11}$$

3. Methodology

In this paper, we focus on estimating the DOAs $\{\theta_1, \theta_2, \ldots, \theta_K\}$ of coherent signals from the received array data matrix, Y, contaminated by α-stable distribution noise. First, a novel operator called CEGC is defined. The boundedness of the CEGC operator is proven to ensure the effectiveness of the proposed method. Subsequently, a coherent DOA estimation method based on CEGC and Toeplitz approximation is derived in detail. The major implementation steps of our proposed method are listed at the end of this section.

3.1. CEGC

Conventional subspace-based DOA estimation methods are based on EVD or SVD of the data covariance matrix, which will fail under α-stable distribution noise since the data statistics of order greater than or equal to two are unbounded in this environment. To overcome this drawback, several modified operators are proposed, of which the FLOS [33] is a typical example. However, the FLOS-based methods rely on prior knowledge of the impulsive noise to select appropriate parameter and require large sample sizes to meet a satisfactory performance. This motivates us to develop more effective operators to deal with impulsive noise.

Recently, a local similarity measurement called correntropy has been proposed [41,42] and has become popular in the area of non-Gaussian signal processing [43–45]. Compared to the FLOS, correntropy can exploit more intrinsic information about infinite statistical moments of the signal and deal with outliers without prior knowledge of the noise. The correntropy of two random variables X and Y is defined as:

$$C_{\sigma}(X, Y) = \mathrm{E}[\kappa_{\sigma}(X - Y)] \tag{12}$$

where $\kappa_{\sigma}(\cdot)$ represents the kernel function and σ is the kernel size. Utilizing data samples $\{(x_i, y_i)\}_{i=1}^{N}$, correntropy can be estimated as follows:

$$\hat{C}_{\sigma}(X, Y) = \frac{1}{N}\sum_{i=1}^{N}\kappa_{\sigma}(x_i - y_i) \tag{13}$$

As a similarity measure between two random variables, correntropy can be regarded as a generalization of the conventional Pearson correlation [41]. Introducing nonlinear mapping by kernel function, correntropy can transform data from the input space to an infinite dimensional, reproducing kernel Hilbert space and effectively eliminating the adverse effect of outliers.

Moreover, the concept of generalized covariance (GC) [46] is introduced to improve the DOA estimation performance in the presence of α-stable distribution noise, since conventional covariance does not converge in this environment. In fact, a series of existing concepts such as FLOS, hyperbolic tangent, and correntropy can unify in the name of GC. The GC of two random variables, X and Y, is defined as:

$$R^{\mathrm{GC}}(X,Y) = \mathrm{E}\left[\frac{g_1(X)}{h_1(X,Y)} \cdot \frac{g_2(X)}{h_2(X,Y)}\right] \tag{14}$$

where $g_1(\cdot)$ and $g_2(\cdot)$ represent single-variable functions. $h_1(\cdot,\cdot)$ and $h_2(\cdot,\cdot)$ represent dual-variable functions, however, both can also be single-variable functions or even constants in some cases.

Inspired by the advantages of correntropy and GC, a novel operator called CEGC is proposed and defined as follows:

$$\overline{R} = \mathrm{E}\left[\mathrm{e}^{-\frac{|X|+|Y|}{\sigma}} XY\right] \tag{15}$$

where the kernel size $\sigma > 0$.

The CEGC operator retains the conventional correlation term and utilizes the exponential kernel to provide further outlier suppression capabilities to adapt to an intensive impulsive noise environment. Furthermore, it can be regarded as a specific case of GC based on the generalized exponential kernel function. In this case, $g_1(X) = X$, $g_2(Y) = Y$, $h_1(\cdot,\cdot) = \mathrm{e}^{-|X|/\sigma}$, $h_2(\cdot,\cdot) = \mathrm{e}^{-|Y|/\sigma}$. To ensure the effectiveness of the proposed method, we prove the boundedness of the CEGC operator.

Theorem 1. *If X and Y are two independent and identically distributed SαS random variables, the CEGC between X and Y is bounded.*

Proof of Theorem 1. We can obtain the CEGC between X and Y as Equation (15). It is apparent that $XY \leq [\max(|X|,|Y|)]^2$. Assuming $|X| \geq |Y|$, we obtain:

$$\begin{aligned}
|\overline{R}| & \leq \mathrm{E}\left[\mathrm{e}^{-\frac{|X|+|Y|}{\sigma}}|X|^2\right] \\
& \leq \mathrm{E}\left[\mathrm{e}^{-\frac{|X|}{\sigma}}|X|^2\right]
\end{aligned} \tag{16}$$

Substituting the characteristic function (11) into (16), we obtain:

$$\begin{aligned}
|\overline{R}| & \leq \mathrm{E}\left[\mathrm{e}^{-\frac{|X|}{\sigma}}|X|^2\right] \\
& = \frac{1}{2\pi}\int_{-\infty}^{+\infty}\int_{-\infty}^{+\infty}\mathrm{e}^{-\frac{|X|}{\sigma}}|X|^2\mathrm{e}^{\mathrm{j}\mu\omega-\gamma|\omega|^\alpha}\mathrm{e}^{-\mathrm{j}\omega X}\mathrm{d}X\mathrm{d}\omega \\
& \leq \frac{1}{\pi}\int_{0}^{+\infty}\int_{-\infty}^{+\infty}\mathrm{e}^{-\frac{X}{\sigma}}X^2\mathrm{e}^{-\gamma|\omega|^\alpha}\mathrm{d}\omega\mathrm{d}X \\
& = \frac{1}{\pi}\int_{0}^{+\infty}\mathrm{e}^{-\frac{X}{\sigma}}X^2\mathrm{d}X\int_{-\infty}^{+\infty}\mathrm{e}^{-\gamma|\omega|^\alpha}\mathrm{d}\omega
\end{aligned} \tag{17}$$

where $\int_{-\infty}^{+\infty}\mathrm{e}^{-\gamma|\omega|^\alpha}\mathrm{d}\omega = 2\int_{0}^{+\infty}\mathrm{e}^{-\gamma\omega^\alpha}\mathrm{d}\omega = \frac{2}{\alpha}\gamma^{-\frac{1}{\alpha}}\Gamma\left(\frac{1}{\alpha}\right) = h$ and $\Gamma(x) = \int_{0}^{+\infty}t^{x-1}\mathrm{e}^{-t}\mathrm{d}t$ denotes the gamma function.

Next, (17) can be simplified as:

$$
\begin{aligned}
|\overline{R}| \;&\leq\; \tfrac{h}{\pi} \int\limits_{0}^{+\infty} e^{-\frac{X}{\sigma}} X^2 \mathrm{d}X \\
&= \tfrac{2h\sigma^3}{\pi} < +\infty
\end{aligned}
\tag{18}
$$

According to (18), we can infer that the CEGC between X and Y is bounded. Thus ends the proof. $\square$

In the next section, the CEGC is utilized to estimate the DOA rather than conventional correlation in the covariance matrix.

3.2. Proposed Method

According to the received signal model (7) and assuming that the noise is independent of the signals, the data covariance matrix, $\boldsymbol{R_Y}$, can be written as:

$$
\begin{aligned}
\boldsymbol{R_Y} \;&= \mathrm{E}\left\{ \boldsymbol{Y}\boldsymbol{Y}^{\mathrm{H}} \right\} \\
&= \boldsymbol{A}\mathrm{E}\left\{ \boldsymbol{X}\boldsymbol{X}^{\mathrm{H}} \right\}\boldsymbol{A}^{\mathrm{H}} + \mathrm{E}\left\{ \boldsymbol{W}\boldsymbol{W}^{\mathrm{H}} \right\} \\
&= \boldsymbol{A}\boldsymbol{R_X}\boldsymbol{A}^{\mathrm{H}} + E\left\{ \boldsymbol{W}\boldsymbol{W}^{\mathrm{H}} \right\}
\end{aligned}
\tag{19}
$$

Conventional subspace-based methods must perform EVD or SVD of the data covariance matrix. When the signal sources are coherent, the source covariance matrix, $\boldsymbol{R_X}$, is rank deficient, i.e., $\boldsymbol{R_X}$ is a singular matrix and the rank of $\boldsymbol{R_X}$ is lower than the number of signal source, K. Therefore, conventional subspace-based methods cannot produce accurate DOA estimations and modified solutions should be used to resolve this situation.

Compared with SS-based methods, the TAM [20–27] method is an effective alternative to resolve coherent signals, since it does not reduce the effective aperture of the array and is capable of achieving higher resolution. However, these methods will fail under α-stable distributed noise because they are developed based on second-order statistics, which are unbounded under α-stable distributed noise.

Combined with the operator CEGC described in Section 3.1, we can construct the pseudo-covariance matrix, $\overline{\boldsymbol{R}}_Y$, of the received signal, $\boldsymbol{Y}$, as:

$$
\overline{\boldsymbol{R}}_Y =
\begin{bmatrix}
\overline{R}_{1,1} & \overline{R}_{1,2} & \cdots & \overline{R}_{1,M} \\
\overline{R}_{2,1} & \overline{R}_{2,2} & \cdots & \overline{R}_{2,M} \\
\vdots & \vdots & \ddots & \vdots \\
\overline{R}_{M,1} & \overline{R}_{M,2} & \cdots & \overline{R}_{M,M}
\end{bmatrix}
\tag{20}
$$

where:

$$
\overline{R}_{i,j} = \overline{R}\left(y_i, y_j{}^{*}\right) = \frac{1}{N} \sum_{n=1}^{N} e^{-\frac{|y_i| + |y_j{}^{*}|}{\sigma}} y_i y_j{}^{*}
\tag{21}
$$

Furthermore, to circumvent problems due to signal coherence, we perform Toeplitz approximation on $\overline{\boldsymbol{R}}_Y$ and construct a Toeplitz matrix, $\boldsymbol{R}_{\mathrm{Top}}$, as:

$$
\boldsymbol{R}_{\mathrm{Top}} =
\begin{bmatrix}
R_{\mathrm{Top}}(0) & R_{\mathrm{Top}}(1) & \cdots & R_{\mathrm{Top}}(M-1) \\
R_{\mathrm{Top}}(-1) & R_{\mathrm{Top}}(0) & \cdots & R_{\mathrm{Top}}(M-2) \\
\vdots & \vdots & \ddots & \vdots \\
R_{\mathrm{Top}}(1-M) & R_{\mathrm{Top}}(2-M) & \cdots & R_{\mathrm{Top}}(0)
\end{bmatrix}
\tag{22}
$$

where:

$$
R_{\mathrm{Top}}(m) =
\begin{cases}
\dfrac{1}{M-m} \sum\limits_{i=1}^{M-m} \overline{R}_{i,i+m}, & 0 \leq m < M \\[2ex]
\dfrac{1}{M+m} \sum\limits_{i=1}^{M+m} \overline{R}_{i-m,i}, & -M < m \leq 0
\end{cases}
\tag{23}
$$

Inspired by the SS-based methods, the FBSS technique can be applied for effective utilization of the data matrix, and we obtain:

$$\overline{R}_{\text{Top}} = \frac{1}{2}\left(R_{\text{Top}} + J_M R_{\text{Top}}^* J_M\right) \tag{24}$$

where J_M denotes the exchange matrix whose components are zeros except for components on the anti-diagonal. Meanwhile, iterative algorithms [21,22] can also be applied to estimate $\overline{R}_{\text{Top}}$ to further improve the performance of the proposed method.

By performing EVD of $\overline{R}_{\text{Top}}$, we obtain:

$$\overline{R}_{\text{Top}} = U_{\text{S}} \Sigma_{\text{S}} U_{\text{S}}^{\text{H}} + U_{\text{N}} \Sigma_{\text{N}} U_{\text{N}}^{\text{H}} \tag{25}$$

where Σ_{S} and Σ_{N} are the diagonal matrices with the K largest eigenvalues and the remaining $M - K$ smaller eigenvalues of $\overline{R}_{\text{Top}}$, respectively. U_{S} and U_{N} are the matrices composed of eigenvectors corresponding to Σ_{S} and Σ_{N}, and span the signal and noise subspace of $\overline{R}_{\text{Top}}$, respectively.

Furthermore, conventional subspace-based methods can be applied to estimate the DOA. We can construct the spatial spectrum based on the classical MUSIC algorithm as:

$$S_{\text{Top}}(\theta) = \frac{1}{a^{\text{H}}(\theta) U_{\text{N}} U_{\text{N}}^{\text{H}} a(\theta)}, \quad -\frac{\pi}{2} \le \theta \le \frac{\pi}{2} \tag{26}$$

By searching K largest peaks of (26), we obtain the DOA estimation $\{\hat{\theta}_1, \hat{\theta}_2, \ldots, \hat{\theta}_K\}$. At this point, we have achieved the proposal for coherent DOA estimation under impulsive noise. The major implementation steps of our proposed method are summarized as follows:

Step 1: Use the array received signal matrix (6) as input to construct the pseudo-covariance matrix, $\overline{R}_Y$ based on (20) and (21).

Step 2: Perform Toeplitz approximation on $\overline{R}_Y$ based on (22) and (23) to construct a Toeplitz matrix, R_{Top}.

Step 3: Construct a modified matrix, $\overline{R}_{\text{Top}}$ based on (24).

Step 4: Perform the EVD of $\overline{R}_{\text{Top}}$ to obtain the eigenvectors, U_{N}, corresponding to the noise subspace.

Step 5: Calculate the spatial spectrum function (26) and search K largest peaks to estimate the DOA of coherent sources.

4. Simulation

In this section, the DOA estimation performance of the proposed method will be evaluated through comprehensive simulations. The simulation results will be analyzed in detail.

We consider a ULA with $M = 10$ sensors whose inter-element spacings are set as a half wavelength. Assume K coherent narrow band signals are located in the far-field of arrays. The number of snapshots is $N = 500$ except in Section 4.4.

Since the typical signal-to-noise ratio will diverge under $S\alpha S$ noise, the generalized signal-to-noise ratio (GSNR) [28] is employed to measure noise intensity and is defined as:

$$\text{GSNR} = 10 \log_{10} \frac{P_s}{\gamma} \tag{27}$$

where P_s is the power of signal and γ is the dispersion parameter of $S\alpha S$ noise.

The proposed method is compared to the FBSS method [13], TAM method [20], FLOM-SS method [37], PFLOM-SS method [39], and CRCO-SS method [40]. For SS-based methods, the number of sensors in the subarray is $M_1 = 6$. The performance of different algorithms is evaluated by two quantities called probability of resolution (PR) and root-mean-square error (RMSE).

In the experiments, a successful resolution of DOA is defined as:

$$\left|\hat{\theta}_k(l) - \theta_k\right| \le 2^\circ, k = 1, \ldots, K \tag{28}$$

where $\hat{\theta}_k(l)$ are the estimated DOA values of the kth target in the lth Monte-Carlo trial. Therefore, the PR is defined as the ratio of the number of successful resolutions to the number of Monte-Carlo trials.

The RMSE is defined as follows:

$$\text{RMSE} = \sqrt{\frac{1}{KL} \sum_{k=1}^{K} \sum_{l=1}^{L} \left|\hat{\theta}_k(l) - \theta_k\right|^2} \tag{29}$$

where L is the number of Monte Carlo trials. Unless otherwise stated, every simulation will carry out 200 Monte Carlo trials.

The related parameters for the simulations are listed in Table 1.

Table 1. Simulation Conditions and Parameter Settings.

Simulations	DOA (Degree)	GSNR (dB)	α	Number of Snapshots
4.1	$(-10, 30, 50)$	0	1.3	500
4.2	$(10, 30)$	$[-5, 15]$	1.3	500
4.3	$(10, 30)$	0	$[1.0, 2.0]$	500
4.4	$(10, 30)$	0	1.3	$[100, 1000]$

4.1. Spatial Spectrums Comparison

In this simulation, we will compare the spectrograms of six candidate methods under a relatively severe $S\alpha S$ noise environment ($\alpha = 1.3$, GSNR = 0 dB). Three coherent signals are located at $(-10^\circ, 30^\circ, 50^\circ)$, which are represented by red dashed lines in Figure 1. The spectrograms of FBSS, TAM, FLOM-SS, PFLOM-SS, CRCO-SS, and the proposed method are shown in Figure 1a–f, respectively. Every figure contains 10 Monte Carlo trials of spatial spectrum.

Figure 1a,b are the spectrograms of FBSS and TAM, respectively. As expected, these two algorithms cannot function properly in the presence of impulsive noise. Three DOAs can hardly be resolved. The FLOM-SS, PFLOM-SS, and CRCO-SS methods are shown in Figure 1c–e, respectively. They can alleviate the impact of impulse noise on DOA estimation. However, the accuracy and stability of the algorithms must be improved. Meanwhile, it can be seen from Figure 1f that the proposed method has the highest performance spectrograms and all DOAs can be resolved easily.

In the following simulations, more numerical results will be given to compare these methods.

4.2. Experiment Results vs. GSNRs

This simulation will focus on the performance comparison with a wide range of GSNRs. Experiment results can be found in Figure 2. Detailed parameters can be found in Table 1.

The PR of all candidate methods are shown in Figure 2a. We find that the performances of PR are improved with the increase of GSNRs. For moderate impulsive noise environments (GSNR > 5 dB), most methods show effective performances except for SS and TAM methods. These two methods are developed based on Gaussian noise assumptions and cannot accurately estimate DOA under impulsive noise. With the decrease of GSNR, the PR of FLOM-SS, PFLOM-SS, and CRCO-SS decrease rapidly. When GSNR = −5 dB, the PR of these three methods are all below 0.1. This indicates that the SS-variant methods

cannot resolve DOA in intense impulsive noise environment. Meanwhile, the proposed method has relatively high PR, even when GSNR is fairly low.
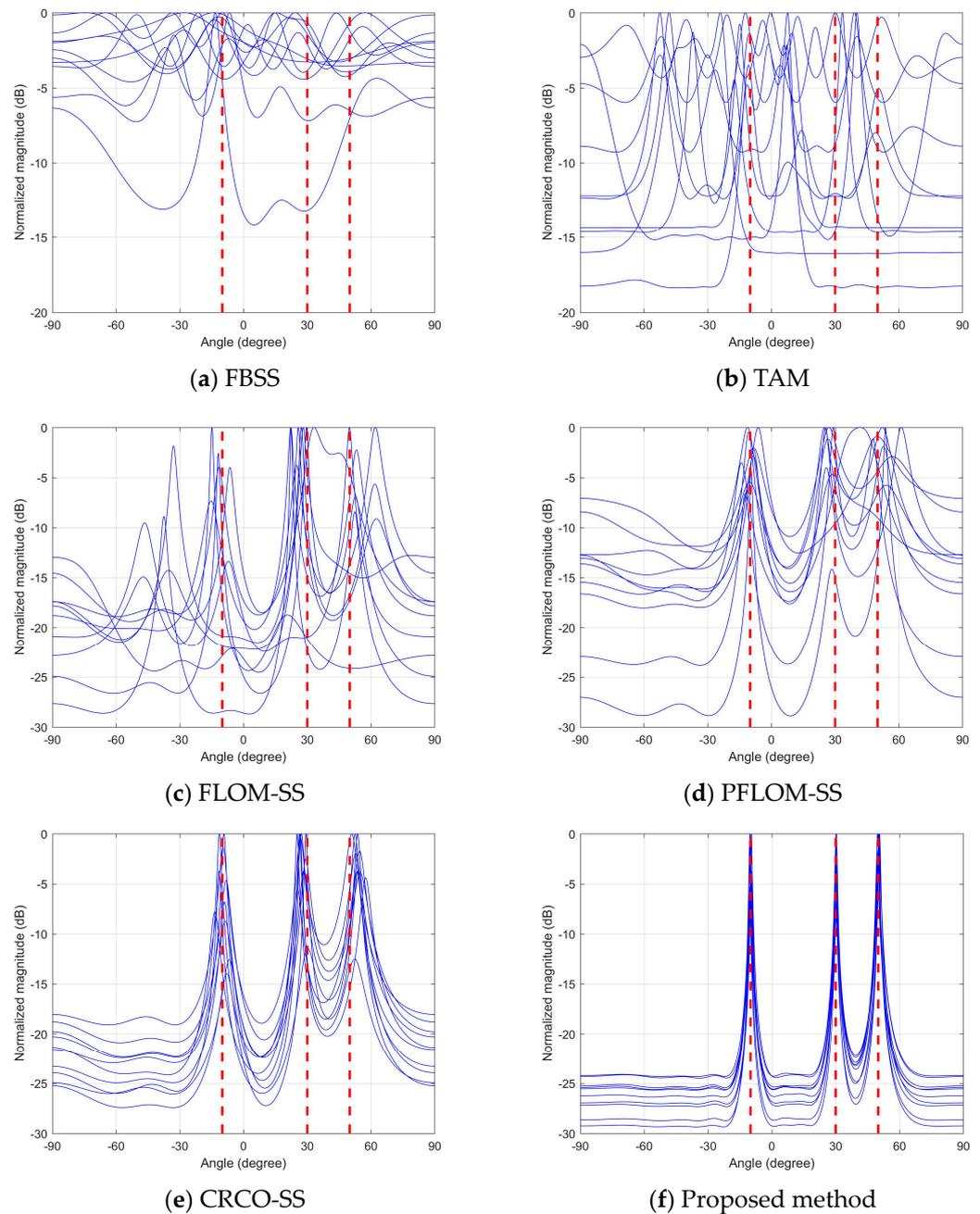

Figure 1. Spatial spectrograms comparison.

To further explore the performance, the RMSE of DOA estimation using different methods are compared in Figure 2b. The FBSS and TAM methods can achieve low RMSE results only when GSNR is high enough. The RMSE of three SS-variant methods increase rapidly when GSNR < 0 dB. Among all candidate methods, the proposed method has the most effective RMSE result.

4.3. Experiment Results vs. Characteristic Exponents α

This simulation will focus on the performance comparison with a wide range of the characteristic exponent α. PR and RMSE results can be found in Figure 3. Detailed parameters can be found in Table 1.

(**a**) PR　　　　　　　　　　　　　　　　　　　(**b**) RMSE
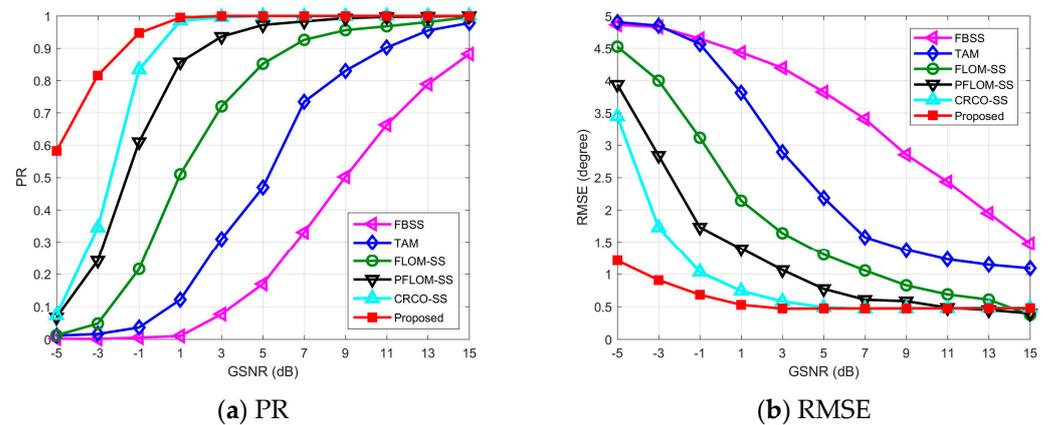
Figure 2. Experimental results vs. GSNRs.

(**a**) PR　　　　　　　　　　　　　　　　　　　(**b**) RMSE
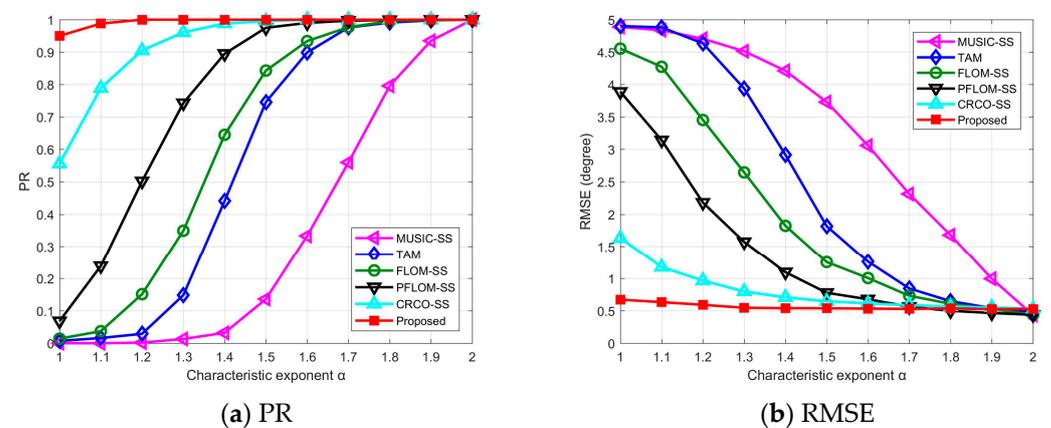
Figure 3. Experimental results vs. characteristic exponent α.

From Figure 3a, we can conclude that all candidate methods can successfully resolve the DOA when $\alpha = 2$, which indicates the validity of all methods under Gaussian noise. With the decrease of α, the impulsiveness of $S\alpha S$ noise is gradually enhanced and the performance of FBSS and TAM deteriorate significantly. The FLOM-SS and PFLOM-SS can achieve high PR when $\alpha > 1.5$ and degrade severely when α approaches 1.0. This is because FLOS-based methods need prior knowledge of the impulsive noise for a satisfactory performance and cannot resist intense impulsive noise. The proposed method outperforms other candidate methods and has the most effective PR result.

Figure 3b is the RMSE results of candidate methods. We find that the RMSE curve of the proposed method fluctuates slightly even when α approaches 1.0. Three SS-variant methods can work well in moderately impulsive noise environments. The RMSE of FBSS and TAM methods increase rapidly with the decrease of α, which shows their vulnerability in impulsive noise environments.

4.4. Experiment Results vs. Number of Snapshots

In this simulation, we evaluate the algorithm performance against the number of snapshots, where $\alpha = 1.3$ and GSNR $= 0$ dB are set. Experiment results can be found in Figure 4. Detailed parameters can be found in Table 1.

As expected, the FBSS and TAM algorithm cannot function properly in the presence of impulsive noise and the number of snapshots has little effect on their performance. For FLOM-SS, PFLOM-SS, and CRCO-SS, the performance improves with the increase of snapshots and towards stability when the number of snapshots is greater than 500. This indicates that a certain number of snapshots are needed to reach satisfactory performance

of the algorithms. Meanwhile, the proposed method requires fewer snapshots to achieve stable performance and the results of PR and RMSE outperform other candidate methods.
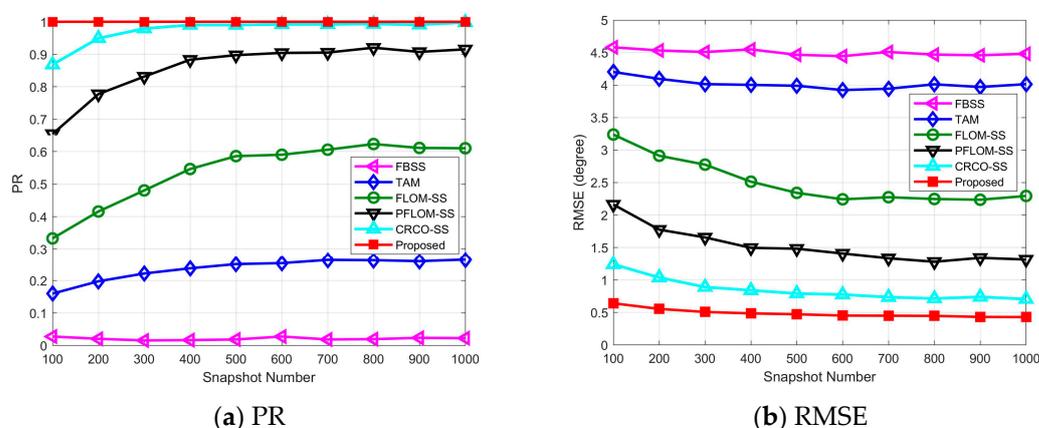

Figure 4. Experimental results vs. number of snapshots.

5. Conclusions

In this paper, we have considered the problem of coherent DOA estimation under α-stable distributed noise. A novel operator termed CEGC was defined first. To ensure the effectiveness of the proposed method under α-stable distributed noise, the proof of boundedness was also provided. Later, we constructed a modified covariance matrix based on CEGC operators and Toeplitz approximation. The modified covariance matrix can be applied to subspace-based methods to estimate the DOA of coherent sources. Finally, multiple simulations were carried out to evaluate the performance of the different methods. Simulation results demonstrate that the proposed method outperforms other existing methods in various α-stable distributed noise environments, even in the case of intense impulsive noise and low snapshot numbers. More array models and computationally efficient methods will be considered in our future works.

Author Contributions: Conceptualization, J.D. and T.Q.; methodology, J.D.; software, J.D., S.L., Q.T. and J.Z.; validation, J.D., S.L., Q.T. and J.Z.; writing—original draft preparation, J.D.; writing—review and editing, J.D., T.Q., S.L., Q.T. and J.Z. All authors have read and agreed to the published version of the manuscript.

Institutional Review Board Statement: Not applicable.

Data Availability Statement: The data are available from the corresponding author upon reasonable request.

Conflicts of Interest: The authors declare no conflict of interest.

References

1. Xu, F.; Morency, M.W.; Vorobyov, S.A. DOA Estimation for Transmit Beamspace MIMO Radar via Tensor Decomposition With Vandermonde Factor Matrix. *IEEE Trans. Signal Process.* **2022**, *70*, 2901–2917. [CrossRef]
2. Zhang, B.; Hou, X.; Yang, Y. Robust Underwater Direction-of-Arrival Tracking with Uncertain Environmental Disturbances Using a Uniform Circular Hydrophone Array. *J. Acoust. Soc. Am.* **2022**, *151*, 4101–4113. [CrossRef]
3. Pan, M.; Liu, P.; Liu, S.; Qi, W.; Huang, Y.; You, X.; Jia, X.; Li, X. Efficient Joint DOA and TOA Estimation for Indoor Positioning With 5G Picocell Base Stations. *IEEE Trans. Instrum. Meas.* **2022**, *71*, 1–19. [CrossRef]
4. Ruan, N.; Wang, H.; Wen, F.; Shi, J. DOA Estimation in B5G/6G: Trends and Challenges. *Sensors* **2022**, *22*, 5125. [CrossRef] [PubMed]

5. Wang, Z.; Zhang, F.; Li, S.; Jin, B. Exploiting Passive Beamforming of Smart Speakers to Monitor Human Heartbeat in Real Time. In Proceedings of the 2021 IEEE Global Communications Conference (GLOBECOM), Madrid, Spain, 7–11 December 2021. [CrossRef]

6. Krim, H.; Viberg, M. Two Decades of Array Signal Processing Research: The Parametric Approach. *IEEE Signal Process. Mag.* **1996**, *13*, 67–94. [CrossRef]

7. Schmidt, R. Multiple Emitter Location and Signal Parameter Estimation. *IEEE Trans. Antennas Propag.* **1986**, *34*, 276–280. [CrossRef]

8. Roy, R.; Kailath, T. ESPRIT-Estimation of Signal Parameters via Rotational Invariance Techniques. *IEEE Trans. Acoust. Speech Signal Process.* **1989**, *37*, 984–995. [CrossRef]

9. Viberg, M.; Ottersten, B.; Kailath, T. Detection and Estimation in Sensor Arrays Using Weighted Subspace Fitting. *IEEE Trans. Signal Process.* **1991**, *39*, 2436–2449. [CrossRef]

10. Stoica, P.; Nehorai, A. MUSIC, Maximum Likelihood, and Cramer-Rao Bound. *IEEE Trans. Acoust. Speech Signal Process.* **1989**, *37*, 720–741. [CrossRef]

11. Evans, J.E.; Sun, D.F.; Johnson, J.R. *Application of Advanced Signal Processing Techniques to Angle of Arrival Estimation in ATC Navigation and Surveillance Systems*; Massachusetts Inst of Tech Lexington Lincoln Lab: Lexington, MA, USA, 1982.

12. Shan, T.J.; Wax, M.; Kailath, T. On Spatial Smoothing for Direction-of-Arrival Estimation of Coherent Signals. *IEEE Trans. Acoust. Speech Signal Process.* **1985**, *33*, 806–811. [CrossRef]

13. Williams, R.T.; Prasad, S.; Mahalanabis, A.K.; Sibul, L.H. An Improved Spatial Smoothing Technique for Bearing Estimation in a Multipath Environment. *IEEE Trans. Acoust. Speech Signal Process.* **1988**, *36*, 425–432. [CrossRef]

14. Pillai, S.U.; Kwon, B.H. Forward/Backward Spatial Smoothing Techniques for Coherent Signal Identification. *IEEE Trans. Acoust. Speech Signal Process.* **1989**, *37*, 8–15. [CrossRef]

15. Li, J. Improved Angular Resolution for Spatial Smoothing Techniques. *IEEE Trans. Signal Process.* **1992**, *40*, 3078–3081. [CrossRef]

16. Pham, G.-T.; Loubaton, P.; Vallet, P. Performance Analysis of Spatial Smoothing Schemes in the Context of Large Arrays. *IEEE Trans. Signal Process.* **2016**, *64*, 160–172. [CrossRef]

17. Du, W.; Kirlin, R.L. Improved Spatial Smoothing Techniques for DOA Estimation of Coherent Signals. *IEEE Trans. Signal Process.* **1991**, *39*, 1208–1210. [CrossRef]

18. Dong, M.; Zhang, S.; Wu, X.; Zhang, H. A High Resolution Spatial Smoothing Algorithm. In Proceedings of the 2007 International Symposium on Microwave, Antenna, Propagation and EMC Technologies for Wireless Communications, Hangzhou, China, 16–17 August 2007. [CrossRef]

19. Pan, J.; Sun, M.; Wang, Y.; Zhang, X. An Enhanced Spatial Smoothing Technique with ESPRIT Algorithm for Direction of Arrival Estimation in Coherent Scenarios. *IEEE Trans. Signal Process.* **2020**, *68*, 3635–3643. [CrossRef]

20. Kung, S.; Lo, C.; Foka, R. A Toeplitz Approximation Approach to Coherent Source Direction Finding. In Proceedings of the ICASSP '86. IEEE International Conference on Acoustics, Speech, and Signal Processing, Tokyo, Japan, 7–11 April 1986. [CrossRef]

21. Wikes, D.M.; Hayes, M.H. Iterated Toeplitz Approximation of Covariance Matrices. In Proceedings of the ICASSP-88, International Conference on Acoustics, Speech, and Signal Processing, New York, NY, USA, 11–14 April 1988. [CrossRef]

22. Chen, Y.-M.; Lee, J.-H.; Yeh, C.-C.; Mar, J. Bearing Estimation without Calibration for Randomly Perturbed Arrays. *IEEE Trans. Signal Process.* **1991**, *39*, 194–197. [CrossRef]

23. Han, F.; Zhang, X. An ESPRIT-like Algorithm for Coherent DOA Estimation. *IEEE Antennas Wirel. Propag. Lett.* **2005**, *4*, 443–446. [CrossRef]

24. Qian, C.; Huang, L.; Zeng, W.-J.; So, H.C. Direction-of-Arrival Estimation for Coherent Signals without Knowledge of Source Number. *IEEE Sens. J.* **2014**, *14*, 3267–3273. [CrossRef]

25. Zhang, W.; Han, Y.; Jin, M.; Qiao, X. Multiple-Toeplitz Matrices Reconstruction Algorithm for DOA Estimation of Coherent Signals. *IEEE Access* **2019**, *7*, 49504–49512. [CrossRef]

26. Zhang, W.; Han, Y.; Jin, M.; Li, X.-S. An Improved ESPRIT-Like Algorithm for Coherent Signals DOA Estimation. *IEEE Commun. Lett.* **2020**, *24*, 339–343. [CrossRef]

27. Hoang, D.T.; Lee, K. Deep Learning-Aided Coherent Direction-of-Arrival Estimation with the FTMR Algorithm. *IEEE Trans. Signal Process.* **2022**, *70*, 1118–1130. [CrossRef]

28. Nikias, C.L.; Shao, M. Signal Processing with Alpha-Stable Distributions and Applications. In *Adaptive and Learning Systems for Signal Processing, Communications, and Control*; Wiley-Interscience: Hoboken, NJ, USA, 1995; Volume 5.

29. Merchant, N.D.; Andersson, M.H.; Box, T.; Le Courtois, F.; Cronin, D.; Holdsworth, N.; Kinneging, N.; Mendes, S.; Merck, T.; Mouat, J.; et al. Impulsive Noise Pollution in the Northeast Atlantic: Reported Activity during 2015–2017. *Mar. Pollut. Bull.* **2020**, *152*, 110951. [CrossRef] [PubMed]

30. Zhou, Z.; Huang, L.; Christensen, M.G.; Zhang, S. Robust Spectral Analysis of Multi-Channel Sinusoidal Signals in Impulsive Noise Environments. *IEEE Trans. Signal Process.* **2022**, *70*, 919–935. [CrossRef]

31. Novey, M.; Adali, T.; Roy, A. A Complex Generalized Gaussian Distribution—Characterization, Generation, and Estimation. *IEEE Trans. Signal Process.* **2010**, *58*, 1427–1433. [CrossRef]

32. Kozick, R.J.; Sadler, B.M. Maximum-Likelihood Array Processing in Non-Gaussian Noise with Gaussian Mixtures. *IEEE Trans. Signal Process.* **2000**, *48*, 3520–3535. [CrossRef]

33. Shao, M.; Nikias, C.L. Signal Processing with Fractional Lower Order Moments: Stable Processes and Their Applications. *Proc. IEEE* **1993**, *81*, 986–1010. [CrossRef]
34. Visuri, S.; Oja, H.; Koivunen, V. Nonparametric Statistics for DOA Estimation in the Presence of Multipath. In Proceedings of the 2000 IEEE Sensor Array and Multichannel Signal Processing Workshop. SAM 2000 (Cat. No.00EX410), Cambridge, MA, USA, 17 March 2000. [CrossRef]
35. Visuri, S.; Oja, H.; Koivunen, V. Subspace-Based Direction-of-Arrival Estimation Using Nonparametric Statistics. *IEEE Trans. Signal Process.* **2001**, *49*, 2060–2073. [CrossRef]
36. Rupi, M.; Tsakalides, P.; Re, E.D.; Nikias, C.L. Robust Spatial Filtering of Coherent Sources for Wireless Communications. *Signal Process.* **2000**, *80*, 381–396. [CrossRef]
37. Li, H.; He, Y.; Wang, H.; Yang, R. Novel Approaches for DOA Estimation of Coherent Sources in the Presence of Impulsive Noise. In Proceedings of the 2006 CIE International Conference on Radar 2006, Shanghai, China, 16–19 October 2006. [CrossRef]
38. Liu, B.; Zhang, J.; Xu, C. DOA Estimation for Coherent Sources in Impulsive Noise Environments. *J. Netw.* **2014**, *9*, 3237. [CrossRef]
39. Li, S.; Lin, B. On Spatial Smoothing for Direction-of-Arrival Estimation of Coherent Signals in Impulsive Noise. In Proceedings of the 2015 IEEE Advanced Information Technology, Electronic and Automation Control Conference (IAEAC), Chongqing, China, 19–20 December 2015. [CrossRef]
40. Guan, S.; Chen, J.; Li, K.; Zhao, Y. General Correntropy Based DOA Estimation for Coherent Source with Impulsive Noise. In *Proceedings of 2019 Chinese Intelligent Systems Conference*; Lecture Notes in Electrical Engineering; Springer: Singapore, 2019; pp. 159–167. [CrossRef]
41. Santamaria, I.; Pokharel, P.P.; Principe, J.C. Generalized Correlation Function: Definition, Properties, and Application to Blind Equalization. *IEEE Trans. Signal Process.* **2006**, *54*, 2187–2197. [CrossRef]
42. Liu, W.; Pokharel, P.P.; Principe, J.C. Correntropy: Properties and Applications in Non-Gaussian Signal Processing. *IEEE Trans. Signal Process.* **2007**, *55*, 5286–5298. [CrossRef]
43. Luan, S.; Qiu, T.; Zhu, Y.; Yu, L. Cyclic Correntropy and Its Spectrum in Frequency Estimation in the Presence of Impulsive Noise. *Signal Process.* **2016**, *120*, 503–508. [CrossRef]
44. Tian, Q.; Qiu, T.; Cai, R. DOA Estimation for CD Sources by Complex Cyclic Correntropy in an Impulsive Noise Environment. *IEEE Commun. Lett.* **2020**, *24*, 1015–1019. [CrossRef]
45. Dai, J.; Qiu, T.; Tian, Q.; Cai, R. Direction of arrival estimation method using deviation from the median based correntropy under impulsive noise. *J. Signal Process.* **2021**, *37*, 1914–1922. [CrossRef]
46. Luan, S.; Zhao, M.; Gao, Y.; Zhang, Z.; Qiu, T. Generalized Covariance for Non-Gaussian Signal Processing and GC-MUSIC under Alpha-Stable Distributed Noise. *Digit. Signal Process.* **2021**, *110*, 102923. [CrossRef]